4344 *Biochemistry* **2009,** *48,* 4344–4353
DOI:10.1021/bi9004045

BIOCHEMISTRY
including biophysical chemistry & molecular biology
Article

Directed Evolution of a Quorum-Quenching Lactonase from *Mycobacterium avium* subsp. *paratuberculosis* K-10 in the Amidohydrolase Superfamily[†]

Jeng Yeong Chow, Long Wu, and Wen Shan Yew*

Department of Biochemistry, Yong Loo Lin School of Medicine, National University of Singapore, 8 Medical Drive, Singapore 117597

Received March 9, 2009; Revised Manuscript Received April 1, 2009

ABSTRACT: The PLL(PTE-like lactonase)-group of enzymes within the amidohydrolase superfamily hydrolyze *N*-acyl-homoserine lactones (AHLs) that are involved in bacterial quorum-sensing pathways. These enzymes possess the $(\beta/\alpha)_8$-barrel fold and serve as attractive templates for *in vitro* evolution and engineering of quorum-quenching biological molecules that can serve as antivirulence therapeutic agents. Using a quorum-quenching lactonase from *Mycobacterium avium* subsp. *paratuberculosis* K-10 (GI: 41409766) as the initial template for *in vitro* evolution experiments, we enhanced the catalytic efficiency and increased the substrate range of the wild-type enzyme through a single point mutation on the loop at the C-terminal end of the eighth β-strand. This N266Y mutant had an increased value of k_{cat}/K_M of 30- and 32-fold toward 3-oxo-*N*-octanoyl-L-homoserine lactone and *N*-hexanoyl-L-homoserine lactone, respectively; the evolved mutant also exhibited lactonase activity toward 3-oxo-*N*-hexanoyl-L-homoserine lactone and *N*-butyryl-L-homoserine lactone, AHLs that were previously not hydrolyzed by the wild-type enzyme. This article reinforces the evolutionary potential of the $(\beta/\alpha)_8$-barrel fold and highlights the possibility of using quorum-quenching lactonases in the amidohydrolase superfamily as templates for engineering biomolecules of therapeutic use.

The amidohydrolase superfamily of enzymes consists of members bearing a conserved mononuclear or binuclear metal center within a $(\beta/\alpha)_8$-barrel structural scaffold (*1*). This metal center is involved in the activation of a water molecule for nucleophilic attack on an activated scissile bond of the substrate for subsequent hydrolysis; enzymes within this superfamily catalyze hydrolytic reactions on a broad range of substrates bearing ester or amide functional groups with carbon or phosphorus centers (*2*). First described by Holm and Sander in 1997 (*3*), the members of the amidohydrolase superfamily have since expanded to include more than 1600 members, catalyzing more than 30 reactions on a variety of substrates ranging from urea to adenosine to the artificial substrate paraoxon (*1*, *4*). Recently, Tawfik and co-workers described a group of divergently related enzymes within the amidohydrolase superfamily, the phosphotriesterase-like lactonases (PLLs[1]) that hydrolyze quorum-sensing *N*-acyl-homoserine lactones (AHLs) (*5*).

Quorum-sensing is an integral part of microbial interaction, and is responsible for the virulence or pathogenecity of disease-causing bacteria (*6*). Quorum-quenching mechanisms have been evolved by microbes to prevent colonization by other microbial populations (*7*). Many of these quenchers are enzymes such as *N*-acyl-homoserine lactonases that are secreted into the environment to degrade the quorum molecules of competing microbial species, effectively disrupting the quorum-sensing pathways of these foreign populations. Modulation and perturbation of this quorum-sensing pathway has been demonstrated, in principle, to be an effective anti-microbial strategy (*8*). Because of the anti-virulent nature of the mode of disruption, this strategy does not present the selective pressure that always results in the development of resistance in microbes and suggests the possible use of these enzymes as attractive therapeutic biomolecules.

Two orthologues from *Mycobacterium tuberculosis* (PPH) and *Rhodococcus erythropolis* (AhlA) within the PLLs were reported to have proficient lactonase activity; however, these orthologues had low solubility and proved to be difficult templates during expression and purification through heterologous systems (*5*). In this article, we describe the use of an orthologous PLL from *Mycobacterium avium* subsp. *paratuberculosis* K-10 (MCP, GI: 41409766) as a template for *in vitro* evolution of enhanced quorum-quenching activity. Pairwise sequence identities between MCP and the reported PLLs, PPH, and AhlA are 92% and 59%, respectively (a matrix of pairwise sequence identities between MCP and selected members of the amidohydrolase superfamily is detailed in the Supporting Information). Like PPH and AhlA, MCP and members of the PLL group within the amidohydrolase superfamily were predicted to contain (1) a HxH motif at the

[†]This research was supported by grants from the National Medical Research Council and the National Research Foundation of Singapore.

*To whom correspondence should be addressed. Phone: (+65) 6516-8624. Fax: (+65) 6779-1453. E-mail: bchyws@nus.edu.sg.

[1]Abbreviations: AHL, *N*-acyl-homoserine lactone; HSL, homoserine lactone; PLL, PTE-like lactonases; MCP, lactonase from *Mycobacterium avium* subsp. *paratuberculosis* K-10; PPH, lactonase from *Mycobacterium tuberculosis*; AhlA, lactonase from *Rhodococcus erythropolis*; PTE, phosphotriesterase; SsoPox, lactonase from *Sulfolobus sulfataricus*; ATCC, American type Culture Collection; IPTG, isopropyl D-thiogalactopyranoside; ICP-OES, inductively coupled plasma optical emission spectroscopy; RhlR, cognate receptor for *N*-butanoyl-L-homoserine lactone; LuxR, cognate receptor for *N*-(3-oxo-hexanoyl)-L-homoserine lactone.

 Published on Web 4/7/2009

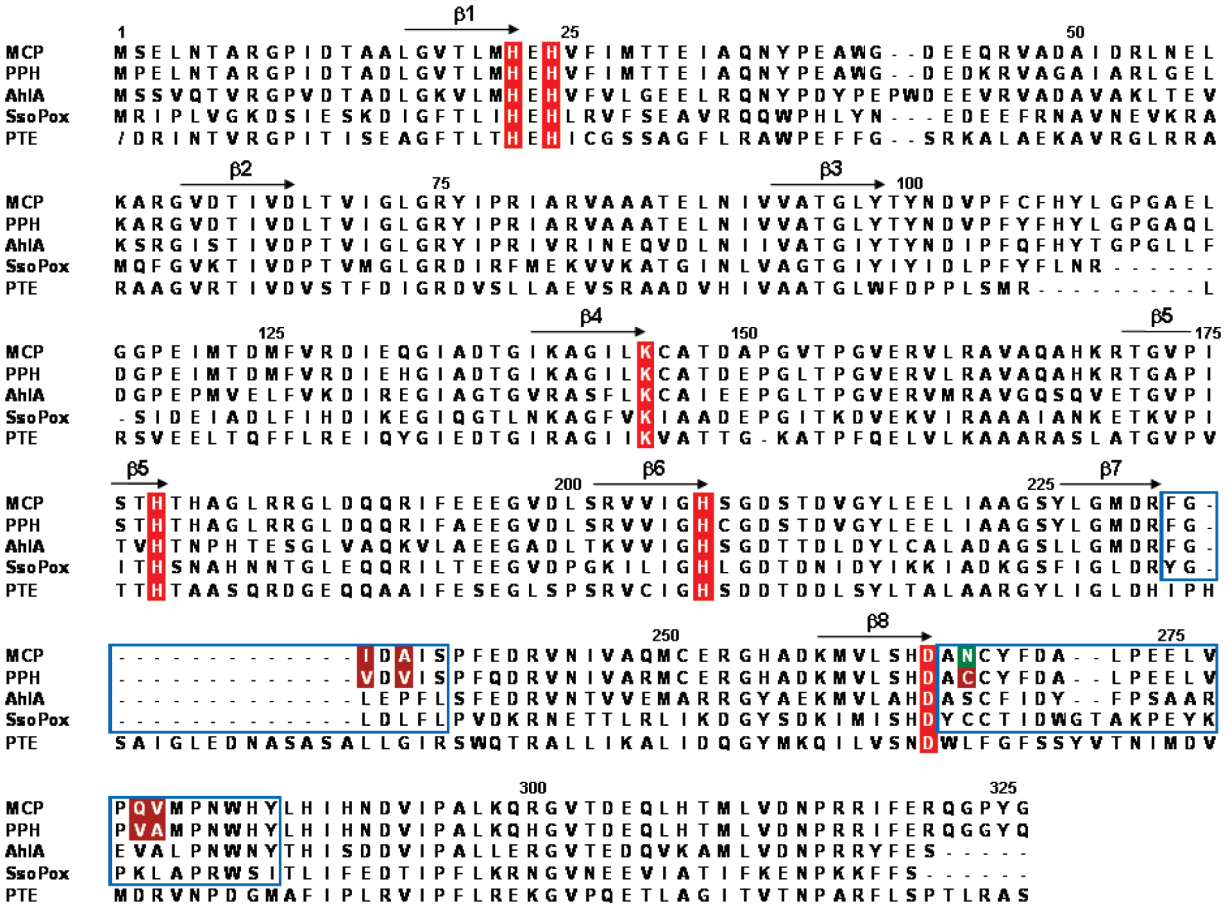

FIGURE 1: Sequence alignment of PLLs from *Mycobacterium avium* subsp. *paratuberculosis* K-10 (MCP), *Mycobacterium tuberculosis* (PPH), *Rhodococcus erythropolis* (AhlA), *Sulfolobus sulfataricus* (SsoPox), and phosphotriesterase from *Pseudomonas diminuta* (PTE) from the amidohydrolase superfamily. The residues highlighted in red are involved in ligand interactions with the binuclear metal center. The residues corresponding to loops at the C-terminal ends of the seventh and eighth β-strands are highlighted by the box in blue. The residues that differ between MCP and PPH in the loops at the C-terminal ends of the seventh and eighth β-strands are highlighted in brown, and the N266 position in MCP is highlighted in green.

end of the first β-strand; (2) His ligands for the binuclear divalent cations at the ends of the fifth and sixth β-strands; (3) a post-translationally carboxylated Lys at the end of the fourth β-strand; and (4) an Asp at the end of the eighth β-strand (Figure 1). We chose MCP as the template for our *in vitro* evolution experiments because of its high solubility and ease of purification. We were able to routinely obtain yields of 30 mg of purified protein per liter of culture; AhlA and PPH have reported yields of 1 mg of purified protein per liter of culture (*5*).

MCP was found to exhibit metal-dependent *N*-acylhomoserine lactonase activity; we determined that Mn^{2+}-reconstituted MCP displayed a substrate preference for medium to long-chain *N*-acyl-homoserine lactones (AHLs). Using a randomly generated library of mutants, we screened for enhanced quorum-quenching activity and identified a mutant, N266Y, with increased catalytic efficiencies (k_{cat}/K_M) toward a number of AHLs. This mutation is located on the loop at the C-terminal end of the eighth β-strand. We explored the plasticity of this loop through saturation mutagenesis experiments and found six other conservative and nonconservative single mutations (Ala, Ser, Thr, Cys, Met, and Phe) with modest increases in activity over the wild-type enzyme. The relative ease of catalytic enhancement through single point mutations and identification of a catalytically plastic substrate-binding loop highlights the potential of using quorum-quenching lactonases in the amidohydrolase superfamily for *in vitro* evolution experiments for engineering therapeutic molecules of biomedical use.

MATERIALS AND METHODS

The substrates *N*-butyryl-DL-homoserine lactone (C4-HSL), *N*-hexanoyl-DL-homoserine lactone (C6-HSL), *N*-(3-oxo-hexanoyl)-L-homoserine lactone (3-oxo-C6-HSL), *N*-heptanoyl-DL-homserine lactone (C7-HSL), *N*-octanoyl-DL-homoserine lactone (C8-HSL), *N*-(3-oxo-octanoyl)-L-homoserine lactone (3-oxo-C8-HSL), *N*-decanoyl-DL-homoserine lactone (C10-HSL), *N*-dodecanoyl-DL-homoserine lactone (C12-HSL), and paraoxon were purchased from Sigma-Aldrich Co. (St. Louis, MO) The chemical structures of these substrates are presented in the Supporting Information. All reagents were of the highest quality grade commercially available.

Cloning, Expression, and Protein Purification of MCP. The gene encoding MCP (GI: 41409766) was PCR amplified from genomic DNA isolated from *Mycobacterium avium* subsp. *paratuberculosis* K-10 (ATCC) using Platinum *Pfx* DNA polymerase (Invitrogen). The PCR reaction (100 μL) contained 1 ng of plasmid DNA, 10 μL of 10X *Pfx* Amplification Buffer, 1 mM $MgSO_4$, 0.4 mM of each dNTP, 40 pmol of each primer (forward primer 5′-GACCTAGCATCAGGCATATGTCAGAACTCA-ATACCGCTCG-3′ and reverse primer 5′-GATCGGCGGG-GGATCCTCACCCATAGGGGCCCTGG-3′), and 5 U of

Platinum *Pfx* DNA polymerase. The gene was amplified using a PTC-0200G Thermal Cycler (Bio-Rad Laboratories), with the following parameters: 94 °C for 2 min followed by 40 cycles of 94 °C for 1 min, 55 °C for 1 min and 15 s, 68 °C for 3 min, and a final extension of 68 °C for 10 min. The amplified gene was cloned into a modified pET-15b vector (Novagen) in which the *N*-terminus contained 10 His residues (kindly provided by Professor John Gerlt, University of Illinois at Urbana−Champaign) (*9*).

The protein was expressed in *E. coli* strain BL21(DE3). Transformed cells were grown at 37 °C in LB broth (supplemented with 100 μg/mL ampicillin) to an OD_{600nm} of 0.6, and isopropyl D-thiogalactopyranoside (IPTG) (0.1 mM) was added to induce protein expression for 16 h. The cells were harvested by centrifugation and resuspended in binding buffer (5 mM imidazole, 0.5 M NaCl, and 20 mM Tris-HCl, pH 7.9) and lysed by sonication. The lysate was cleared by centrifugation, and the His-tagged protein was purified using a column of chelating Sepharose Fast Flow (GE Healthcare Bio-Sciences Corp.) charged with Ni^{2+}. The cell lysate was applied to the column in binding buffer, washed with buffer containing 154 mM imidazole, 0.5 M NaCl, and 20 mM TrisHCl at pH 7.9, and eluted with 100 mM L-histidine, 0.5 M NaCl, 20 mM Tris-HCl at pH 7.9. The N-terminal His-tag was removed with thrombin (GE Healthcare Bio-Sciences Corp.) according to the manufacturer's instructions, and the proteins were purified to homogeneity on a Q Sepharose High Performance column (GE Healthcare Bio-Sciences Corp.) equilibrated with binding buffer (25 mM Tris-HCl at pH 7.9) and eluted with a linear gradient of 0 to 0.5 M elution buffer (1 M NaCl and 25 mM Tris-HCl at pH 7.9).

Preparation of MCP for Metal-Dependency Studies. Purified MCP was dialyzed against storage buffer (100 mM NaCl and 20 mM Tris-HCl at pH 8.0) containing 10 mM ethylene diamine tetraacetic acid (EDTA), followed by dialysis in storage buffer to remove excess EDTA. EDTA-treated MCP was sent for inductively-coupled plasma optical emission spectroscopy (ICP-OES) metal-analysis at the Elemental Analysis Laboratory, Department of Chemistry, National University of Singapore. Metal-reconstituted MCP was prepared by dialysis of EDTA-treated MCP against storage buffer containing 100 μM metal ions (Mg^{2+}, Ca^{2+}, Mn^{2+}, Fe^{2+}, Co^{2+}, Ni^{2+}, Cu^{2+}, and Zn^{2+}). The Mn^{2+}-reconstituted MCP was dialyzed against the storage buffer before ICP-OES analysis.

Kinetic Assays of N-Acyl-homoserine Lactonase Activity. The *N*-acyl-homoserine lactonase activity of MCP was assayed by a continuous spectrophotometric pH indicator assay (described by Chapman and Wong (*10*) to detect the formation of carboxylic acids), using a UV-2550 Spectrophotometer (Shimadzu). The assay (1 mL at 25 °C) contained MCP, 2.5 mM bicine buffer at pH 8.3, 0.08 mM cresol purple (577 nm, $\varepsilon = 12{,}500\ M^{-1}cm^{-1}$), 10 μM of metal ion ($Mg^{2+}$, Ca^{2+}, Mn^{2+}, Fe^{2+}, Co^{2+}, Ni^{2+}, Cu^{2+}, or Zn^{2+}), and 0.025−5 mM AHL substrate (AHL substrates were dissolved in DMSO, and regardless of substrate concentration, the final concentration of organic solvent DMSO was maintained at 1%). Initial rates (v_o) were corrected for the background rate of spontaneous substrate hydrolysis in the absence of enzyme. Kinetic parameters were determined by fitting the initial rates to the Michaelis−Menten equation using Enzfitter (Biosoft). Paraoxonase activity was assayed as previously described by Aubert et al. (*11*), with the following modifications: briefly, the assay (1 mL at 25 °C) contained MCP, 50 mM Tris-HCl at pH 8.0, 10 μM $MnCl_2$, and 0.1−2.5 mM paraoxon (400 nm, $\varepsilon = 17{,}000\ M^{-1}cm^{-1}$, 0.25% methanol). The reaction was monitored spectrophotometrically by following the formation of *p*-nitrophenol at 400 nm.

Bioluminescence Quorum-Quenching Bioassay. To demonstrate the quorum-quenching activity of MCP, we adapted the bioluminescence-based reporter-plasmid biosensor assay developed by Ahmer and co-workers (*12*) as shown in Figure 2. Reporter plasmids with cognate receptors for *N*-butanoyl-L-homoserine lactone (RhlR) or *N*-(3-oxo-hexanoyl)-L-homoserine lactone (LuxR) were transformed into an *sdiA*-deficient *E.coli* strain (the *sdiA* genomic deletion allows normal functioning of the biosensor assay, a kind gift from Professor Brian Ahmer, Ohio State University); a modified pKK-223-3 plasmid (*13*) (kindly provided by Professor John Gerlt, University of Illinois at Urbana−Champaign) bearing the MCP gene was introduced into the reporter strain, and single-colony transformants were streaked onto LB plates supplemented with 100 μg/mL ampicillin, 20 μg/mL tetracycline, 25 μg/mL chloramphenicol, 0.1 mM IPTG, and AHL substrate. The plates were then incubated overnight at 37 °C, and bioluminescence was detected using a LAS-1000 luminescent image analysis system (Fujifilm).

Construction of Site-Specific MCP mutants. The site-directed D264N and D264A mutants of MCP were constructed using the QuikChange kit (Stratagene), verified by sequencing, expressed in the BL21(DE3) *E. coli* cells, and purified as previously described for the wild-type protein. These mutants were also subcloned into the modified pKK-223-3 vector for bioluminescence quorum-quenching assays as previously described.

Directed Evolution of MCP toward Increased Quorum-Quenching Activity. A randomly generated error-prone PCR library of MCP mutants was constructed using the GeneMorph II random mutagenesis kit (Stratagene). Briefly, for each error-prone PCR reaction, 450 ng of MCP template was used to obtain a mutation frequency of ~3.6 mutations per kb (determined by sequencing randomly picked transformants). The mutant PCR product was cloned into the modified pKK-223-3 plasmid and transformed into XL1 Blue *E.coli* cells. Five transformations

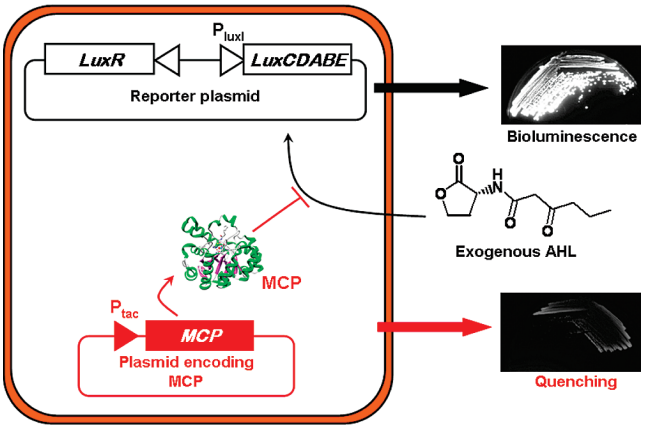

FIGURE 2: Detection of quorum-quenching activity. The *E.coli*-based quorum biosensor constitutively expresses the quorum receptor (LuxR), and in the presence of exogenous AHLs, the quorum receptor−AHL complex would drive the expression of the reporter gene cassette (*LuxCDABE*) through the quorum promoter P_{LuxI}; thus, the presence of exogenous AHLs would result in bioluminescence, as highlighted by the black pathway. In the presence of lactonases (e.g., MCP) expressed by an additional, compatible P_{tac}-driven plasmid, exogenous AHLs would be hydrolyzed to the corresponding acyl-homoserines, resulting in quorum-quenching of bioluminescence, as highlighted by the red pathway.

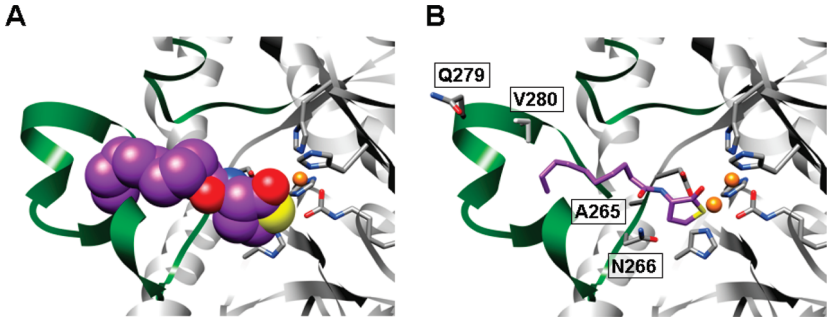

FIGURE 3: Structure of the active site and substrate binding loops of SsoPox. (A) The substrate specificity loops, corresponding to the SsoPox sequences (boxed in blue) in Figure 1, are highlighted in green. The *N*-decanoyl-L-homocysteine thiolactone ligand (magenta) bound in the active site is represented with van der Waal's radii. (B) An *in silico* representation of the MCP residues A265, N266, Q279, and V280 relative to the substrate in the active site. The MCP residues A265, N266, Q279, and V280, corresponding to the SsoPox residues Y257, C258, K273, and L274, respectively, were introduced using the swapaa function in the UCSF Chimera package, from the Resource for Biocomputing, Visualization, and Informatics at the University of California, San Francisco, CA (supported by NIH Grant P41 RR-01081) (*24*).

resulted in a library size of 7×10^5 transformants. The mutant MCP plasmid library was harvested using the QIAprep Miniprep Kit (Qiagen), and transformed into the quorum reporter strain to screen for MCP mutants with increased quorum-quenching activities. Colonies with increased quorum-quenching were picked, and the sequences of the mutants were determined by DNA sequencing.

Construction of Site-Specific Random MCP Libraries. Site-specific random MCP libraries at positions 265, 266, 267, 268, 269, 270, and 279/280 (corresponding to codons on the loop at the C-terminal end of the eighth β-strand) were constructed using the QuikChange method, with the primers for construction of the libraries detailed in the Supporting Information. We routinely obtained a library size of 1×10^4 transformants per transformation. The site-specific random MCP libraries were harvested as previously described, and the randomized codons were verified by DNA sequence analysis. These libraries were similarly transformed into the quorum reporter strain to screen for MCP mutants with increased quorum-quenching activities. Colonies with increased quorum-quenching were picked, and the sequences of the mutants were determined by DNA sequencing.

Construction of MCP-AhlA and MCP-PPH Chimeras. With the expectation that the binuclear metal centers of MCP, AhlA, PPH, and SsoPox are essentially identical, we identified the specificity loops at the C-terminal ends of the seventh and eighth β-strand from a sequence alignment based upon the structure of SsoPox (PDB ID: 2VC7) (*14*); these loops, highlighted in green in Figure 3A, are represented by the sequences boxed in blue in Figure 1. MCP-AhlA and MCP-PPH chimeras were constructed using the QuikChange method, with the primers for construction of the libraries detailed in the Supporting Information. MCP-AhlA and MCP-PPH chimeras were MCP mutants that had their loops at the C-terminal ends of the seventh and/or eighth β-strands replaced with the corresponding loops from AhlA and PPH, respectively (exact sequences are highlighted by the blue box in Figure 1). These chimeras were verified by DNA sequencing and purified as previously described for the wild-type protein.

RESULTS AND DISCUSSION

The biological roles of PLLs within the amidohydrolase superfamily have been proposed to be associated with the quorum-quenching mechanisms of microbes (*5*). Tawfik and co-workers first reported two orthologues of quorum-quenching lactonases from *Rhodococcus erythropolis* (AhlA) and *Mycobacterium tuberculosis* (PPH). Both AhlA and PPH exhibited proficient lactonase activity toward a number of AHLs, while demonstrating low paraoxonase activity; paraoxon is an insecticide component and has been shown to be efficiently hydrolyzed (k_{cat}/K_M of 10^7 $M^{-1}s^{-1}$) by phosphotriesterase (PTE), a divergently related homologue in the amidohydrolase superfamily (*2*, *15*). However, although both AhlA and PPH have reportedly proficient quorum-quenching activities, they proved to be difficult templates for heterologous expression, with protein yields of about 1 mg per liter of culture. In order to use such templates for protein evolution and *in vitro* engineering purposes, we sought to identify other orthologous quorum-quenching PLLs with higher yields through heterologous expression systems.

Identification and Biochemical Characterization of a Quorum-Quenching Lactonase. MCP and PPH have a high sequence identity (92% amino acid sequence identity), differing only in 26 out of 326 amino acids for the complete polypeptide. As such, from the sequence predictions, we expected MCP, an orthologous PLL within the amidohydrolase superfamily, to exhibit lactonase activity toward AHLs. We were able to obtain 30 mg/L of culture of MCP, a 30-fold increase in purified protein yield over the reported yield of PPH. The protein purity was estimated to be greater than 98% as judged from SDS−PAGE analysis. We screened the purified MCP for activity against AHLs in the absence of additional metal ions and detected lactonase activity. As a member of the amidohydrolase superfamily of enzymes, we expected MCP to demonstrate metal dependency for its AHL lactonase activity. To elaborate on the predicted metal dependency, we treated MCP with the divalent metal ion chelating agent, EDTA. EDTA-treated MCP was found to contain 1.0 equiv of iron, 0.05 equiv of manganese, and 0.05 equiv of zinc per active site; we attributed this observation to a possible high affinity of the active site for iron. EDTA-treated MCP retained about 30% of activity compared to non-EDTA-treated MCP. We proceeded to determine the metal dependency of MCP AHL lactonase activity by reconstituting EDTA-treated MCP with the following metal ions: Mg^{2+}, Ca^{2+}, Mn^{2+}, Fe^{2+}, Co^{2+}, Ni^{2+}, Cu^{2+}, and Zn^{2+}. Using 0.4 mM C8-HSL as substrate, we determined that metal-reconstituted MCP exhibited the highest lactonase activity with manganese, followed by zinc (which had 20% less activity than manganese); none of the other metal ions increased lactonase activity above that of EDTA-treated MCP. We used manganese-reconstituted MCP for the rest of our experiments.

Table 1: Kinetic Parameters of MCP and N266Y

	MCP			N266Y			
substrate	k_{cat} (s^{-1})	K_M (mM)	k_{cat}/K_M ($M^{-1}s^{-1}$)	k_{cat} (s^{-1})	K_M (mM)	k_{cat}/K_M ($M^{-1}s^{-1}$)	rel k_{cat}/K_M
C4-HSL	ND[a]	ND	ND	[b]	[b]	11	[c]
C6-HSL	[b]	[b]	23	2.8 ± 0.27	3.8 ± 0.57	730	32
3-oxo-C6-HSL	ND	ND	ND	3.4 ± 0.85	30 ± 8.7	110	[c]
C7-HSL	0.77 ± 0.16	1.8 ± 0.48	430	3.6 ± 0.20	1.2 ± 0.16	3.0×10^3	7.0
C8-HSL	0.83 ± 0.10	0.40 ± 0.082	2.1×10^3	5.4 ± 0.33	0.35 ± 0.065	1.6×10^4	7.6
3-oxo-C8-HSL	0.56 ± 0.12	1.7 ± 0.51	330	9.2 ± 0.68	0.93 ± 0.18	9.9×10^3	30
C10-HSL	0.87 ± 0.18	0.13 ± 0.043	6.7×10^3	2.5 ± 0.072	0.044 ± 0.0041	5.6×10^4	8.4
C12-HSL	0.30 ± 0.025	0.023 ± 0.00085	1.3×10^4	1.3 ± 0.068	0.025 ± 0.0054	5.3×10^4	4.1
paraoxon	$(7.1 \pm 0.95) \times 10^{-3}$	1.7 ± 0.43	4.1	0.065 ± 0.015	2.3 ± 0.94	28	6.8

[a] ND, no detectable activity. [b] Saturation kinetics could not be attained. [c] New substrate with detectable activity.

Manganese-reconstituted MCP was found to contain 1.0 equiv of iron, 0.6 equiv of manganese, and 0.05 equiv of zinc per active site.

Within our expectations, MCP exhibited lactonase activity toward a number of AHL substrates; the values of the kinetic parameters and the identities of the AHL substrates are reported in Table 1. We have shown that MCP demonstrates a substrate preference for medium (k_{cat}/K_M of 2.1×10^3 M^{-1} s^{-1} for C8-HSL) to long-chain (k_{cat}/K_M of 1.3×10^4 M^{-1} s^{-1} for C12-HSL) AHLs; this contrasts with the broad substrate range reported for the PPH orthologue (*5*). MCP also had low paraoxonase activity (k_{cat}/K_M of 4.1 M^{-1} s^{-1} for paraoxon), indicating that, like other members of the PLLs, the native substrate profile of this enzyme does not involve phosphate esters (*5*, *16*).

In Vitro Evolution of the MCP Scaffold for Increased AHL Lactonase Activity. We sought to increase the catalytic efficiency of MCP toward the AHL substrates as well as broaden the AHL substrate range so that it will be useful for further development as an antivirulence therapeutic agent. We used the *E.coli* quorum-sensor strain from Professor Ahmer as a screen to detect quorum-quenching activity: as illustrated in Figure 2, the quorum biosensor detects exogenous AHL molecules and exhibits bioluminescence; in the presence of an additional compatible plasmid that expresses quorum-quenching lactonase, the exogenous AHL molecules would be depleted, and bioluminescence would be quenched. To address the possibility of AHL-sequestration by the lactonases, we transformed the quorum-sensor strain with plasmid-encoding inactive D264N and D264A mutants (Asp 264 is absolutely conserved in PLLs and in PTEs and is located at the ends of the eight β-strand; we obtained protein yields for D264N/A mutants similar to that of wild-type MCP, and we detected no lactonase activity toward the various AHL substrates); we observed no quenching of bioluminescence for the quorum-sensor strain in the presence of inactive D264N/A mutants, while quorum-quenching was evident in the strains transformed with wild-type MCP (Figure 4, panels A and B). We therefore concluded that quenching of bioluminescence was due to the quorum-quenching lactonase activity of MCP. MCP displayed a higher lactonase activity toward C8-HSL over 3-oxo-C8-HSL, and this 6-fold increase in catalytic efficiency translated to an observed higher degree of quorum-quenching/bioluminescence-quenching. These observations led us to believe that we could use this quorum-biosensor bioassay as a platform to screen for increased AHL lactonase activities.

A library of random MCP mutants, constructed by error-prone PCR, was transformed into the quorum biosensor and screened for increased AHL lactonase activity against 100 nM

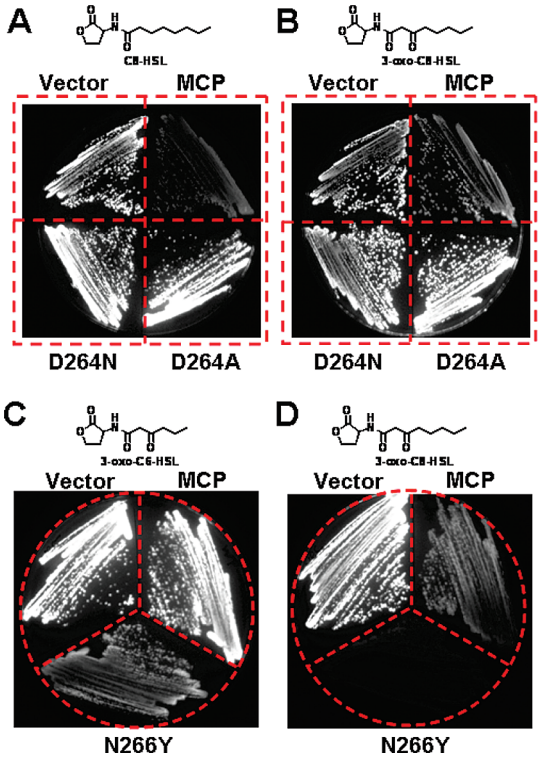

FIGURE 4: Comparison of quorum-quenching by wild-type and mutant MCPs. Wild-type MCP and inactive D264N/A mutants in the presence of 100 nM (A) C8-HSL and (B) 3-oxo-C8-HSL. Clockwise from top-left quadrant: quorum biosensor transformed with vector control, wild-type MCP, and inactive D264A and D264N mutants, respectively. Wild-type and N266Y in the presence of 100 nM (C) 3-oxo-C6-HSL and (D) 3-oxo-C8-HSL. Clockwise from top-left division: quorum biosensor transformed with vector control, wild-type MCP, and N266Y mutant, respectively.

3-oxo-C8-HSL. A typical screen containing colonies of transformants is shown in the Supporting Information; colonies of varying bioluminescence intensities were observed, and colonies displaying strong quenching of bioluminescence were picked and verified by restreaking and comparing with wild-type MCP. From an initial 126 clones that were picked, 9 clones were verified (by restreaking and comparing with wild-type MCP for enhanced bioluminescence quenching) to have improved quenching; these clones were used as templates for a second round of error-prone PCR, and the process was repeated for a third round of mutagenesis and screening. The concentration of 3-oxo-C8-HSL was increased to 1 μM and 10 μM, respectively, for the second and third rounds of *in vitro* evolution. We noticed that

there was a high rate of false positives from the initial screening of clones for enhanced quenching of bioluminescence; we attributed that to the usage of a high-copy pKK223-3-derived plasmid during the screening process. Although the use of a high-copy plasmid could have resulted in varying levels of protein expression (within cells in a clonal expansion) and hence to increased quenching due to higher protein expression levels, we were able to eliminate false-positive clones by a simple restreaking procedure. Perhaps for future *in vitro* evolution of quorum-quenching lactonases, one could use a tightly regulated, tunable-transcription expression vector with an enzyme-degradation tag to reduce intracellular enzyme concentration levels for a more consistent experimental screen (*17*).

After three rounds of screening, we obtained 10 clones that exhibited increased bioluminescence quenching, as compared to that of wild-type MCP. We observed that the N266Y mutation (a single-base change from AAC to TAC at the 266 codon) was present in all of the 10 clones identified after 3 rounds of screening. This convergence led us to select this mutation for further characterization. We constructed the N266Y mutant using the observed single-base mutation and compared its quorum-quenching abilities with the 10 clones identified after 3 rounds of screening. To our surprise, the N266Y mutant exhibited the highest quenching of bioluminescence when compared to that of those clones; apparently, additional mutations acquired through the subsequent rounds of *in vitro* evolution had a deleterious effect on activity when combined with the N266Y mutation. We purified the N266Y mutant and measured its kinetic parameters for hydrolysis of various AHL substrates (Table 1). The enhanced quorum-quenching lactonase activity of the N266Y mutant is shown in Figure 4 (panels C and D).

The N266Y mutation resulted in an increase in catalytic activity for all AHL substrates tested. In comparison to wild-type MCP, this single-point mutant had increased k_{cat} values, decreased K_M values, and overall increases in catalytic efficiencies (k_{cat}/K_M) of 4- to 32-fold (for C12-HSL and C6-HSL, respectively). Most noteworthy, the N266Y mutation resulted in a broadening of AHL substrate specificity, allowing the quorum-quenching lactonase to hydrolyze both C4-HSL and 3-oxo-C6-HSL, substrates that the wild-type MCP did not hydrolyze. Since we used 3-oxo-C8-HSL as a substrate for our *in vitro* evolution experiments, we were not surprised to find that this mutant had one of the highest improvements in lactonase activity toward 3-oxo-C8-HSL; the turnover number (k_{cat}) and catalytic efficiency (k_{cat}/K_M) toward 3-oxo-C8-HSL was enhanced 16- and 30-fold, respectively, relative to those of the wild-type enzyme. Wild-type MCP exhibited promiscuous paraoxonase activity, and serendipitously, we also found that the N266Y mutation led to an increase (of 6.8-fold in k_{cat}/K_M over wild-type MCP) in paraoxonase activity (although compared to PTE, the paraoxonase activity of N266Y would still be considered very low).

Site-Specific Random Mutagenesis of Residues in the Loop at the C-Terminal Ends of the Eighth β-Strand. We noticed that the N266Y mutation resided in the loop ($\beta\alpha$ loop) at the C-terminal end of the eighth β-strand of MCP (Figures 1 and 3B). Since the substrate specificity (and hence catalytic activity) of $(\beta/\alpha)_8$-barrel proteins can be dictated by residues present at the C-terminal ends of the β-strands and the $\beta\alpha$ loops (*1*, *18*), we explored the possibility of uncovering mutations to other residues within this loop that could contribute to further enhancements in AHL lactonase activity beyond that exhibited by the N266Y mutation. We were also fully aware that the size of our library of random MCP mutants was very limited, and we were unable to cover all of the available sequence-function space; thus, we constructed site-specific random MCP libraries at positions 265, 266, 267, 268, 269, and 270 (residues around the N266Y mutation) and screened for mutants with enhanced quorum-quenching activities.

We were unable to identify mutants with increased quorum-quenching activities, relative to the wild-type enzyme, from the C267X, Y268X, F269X, and D270X libraries. We identified four mutants (A265G, A265C, A265H, and A265Y) from the A265X library and six mutants, in addition to N266Y (N266F, N266A, N266C, N266M, N266S, and N266T), from the N266X library that appeared to have increased quorum-quenching activities relative to the wild-type enzyme; the kinetic parameters of these mutants are detailed in Table 2. Upon characterization of the purified A265 mutants, we found that three mutants (A265G, A265H, and A265Y) identified through the screen possessed comparable or lower AHL lactonase activity, relative to that of the wild-type enzyme. We did find that in the A265C mutant, there was detectable AHL lactonase activity for C4-HSL, although the catalytic activities of this mutant toward the medium (C8-HSL and 3-oxo-C8-HSL) and long-chain (C12-HSL) AHLs did not improve, relative to that of the wild-type enzyme.

We were surprised to find six other N266 mutants that had increased AHL lactonase activity, relative to that of the wild-type enzyme; this suggested a certain catalytic plasticity for the $\beta\alpha$ loop at the C-terminal end of the eighth β-strand of MCP. Together with the N266Y mutant, we found a total of seven possible amino acids at the 266 position that resulted in enhanced AHL lactonase activity. Incidentally, serine and cysteine residues at the 266 position (from the N266S and N266C mutants) were observed in the corresponding positions for other PLLs (Figure 1). An *in silico* representation of the possible orientation of the N266 residue, relative to the bound substrate, is shown in Figure 3B. We speculated that, given the relatively close proximity of the N266 residue to the lactone ring of the AHL substrate, appropriate substitutions at this position could result in a more productive substrate binding geometry that resulted in the observed enhancements in AHL lactonase activity. However, the lack of commonality in the chemical identities of the side chains of these amino acids suggested that there are secondary and more remote effects involved. We also noted that none of the additional mutations at the 266 position resulted in AHL lactonase activities above that observed for the N266Y mutant; for ease of comparison, we have listed the fold-differences in catalytic efficiencies (k_{cat}/K_M) of the site-specific mutants relative to the N266Y mutant in Table 3. In a previous study to enhance the promiscuous D-*arabino*-hex-3-ulose 6-phosphate synthase activity of 3-keto-L-gulonate 6-phosphate decarboxylase, observations were made that provided credence to our hypothesis that enhancements in AHL lactonase activity could be a result of productive substrate binding geometries: subtle changes (E112D/T169A substitutions) to residues in the active site resulted in altered (productive) D-ribulose 5-phosphate binding conformations (*19*, *20*). We are currently in the process of obtaining a structural explanation for the enhanced reactivity of the N266Y mutant.

Loop Grafting from AhlA and PPH to MCP. The grafting of active site loops have been employed to effect changes in substrate specificity (*21*, *22*). Since there was a disparity in substrate specificities between MCP, AhlA, and PPH (MCP had no detectable C4-HSL lactonase activity, while the values of

Table 2: Kinetic Parameters of Site-Specific MCP Mutants

	A265G			A265C		
substrate	k_{cat} (s^{-1})	K_M (mM)	k_{cat}/K_M ($M^{-1}s^{-1}$)	k_{cat} (s^{-1})	K_M (mM)	k_{cat}/K_M ($M^{-1}s^{-1}$)
C4-HSL	ND[a]	ND	ND	[b]	[b]	3.3
C8-HSL	[b]	[b]	330	1.66 ± 0.10	1.0 ± 0.11	1.6×10^3
3-oxo-C8-HSL	0.45 ± 0.10	1.8 ± 0.80	250	1.3 ± 0.051	2.3 ± 0.17	570
C12-HSL	0.25 ± 0.023	0.026 ± 0.0097	9.6×10^3	0.54 ± 0.035	0.040 ± 0.0086	1.3×10^4
	A265H			A265Y		
substrate	k_{cat} (s^{-1})	K_M (mM)	k_{cat}/K_M ($M^{-1}s^{-1}$)	k_{cat} (s^{-1})	K_M (mM)	k_{cat}/K_M ($M^{-1}s^{-1}$)
C4-HSL	ND	ND	ND	ND	ND	ND
C8-HSL	[b]	[b]	260	1.0 ± 0.099	0.73 ± 0.14	1.4×10^3
3-oxo-C8-HSL	[b]	[b]	43	0.73 ± 0.062	2.0 ± 0.33	360
C12-HSL	[b]	[b]	1.7×10^3	0.55 ± 0.046	0.043 ± 0.012	1.3×10^4
	N266F			N266A		
substrate	k_{cat} (s^{-1})	K_M (mM)	k_{cat}/K_M ($M^{-1}s^{-1}$)	k_{cat} (s^{-1})	K_M (mM)	k_{cat}/K_M ($M^{-1}s^{-1}$)
C4-HSL	[b]	[b]	2.9	[b]	[b]	10
C8-HSL	3.3 ± 0.43	0.49 ± 0.15	6.6×10^3	4.1 ± 0.33	0.38 ± 0.078	1.1×10^4
3-oxo-C8-HSL	6.5 ± 0.23	2.1 ± 0.14	3.1×10^3	8.9 ± 1.3	4.8 ± 1.0	1.9×10^3
C12-HSL	1.4 ± 0.14	0.061 ± 0.016	2.3×10^4	1.6 ± 0.20	0.094 ± 0.026	1.7×10^4
	N266C			N266M		
substrate	k_{cat} (s^{-1})	K_M (mM)	k_{cat}/K_M ($M^{-1}s^{-1}$)	k_{cat} (s^{-1})	K_M (mM)	k_{cat}/K_M ($M^{-1}s^{-1}$)
C4-HSL	[b]	[b]	6.2	[b]	[b]	9.3
C8-HSL	3.9 ± 0.72	0.83 ± 0.29	4.7×10^3	2.8 ± 1.2	1.6 ± 1.0	1.8×10^3
3-oxo-C8-HSL	6.3 ± 1.2	4.5 ± 1.3	1.4×10^3	3.7 ± 0.43	2.9 ± 0.59	1.3×10^3
C12-HSL	1.4 ± 0.13	0.049 ± 0.014	2.9×10^4	0.87 ± 0.046	0.032 ± 0.0063	2.7×10^4
	N266S			N266T		
substrate	k_{cat} (s^{-1})	K_M (mM)	k_{cat}/K_M ($M^{-1}s^{-1}$)	k_{cat} (s^{-1})	K_M (mM)	k_{cat}/K_M ($M^{-1}s^{-1}$)
C4-HSL	[b]	[b]	6.5	[b]	[b]	7.3
C8-HSL	2.7 ± 0.31	0.35 ± 0.10	7.8×10^3	2.8 ± 0.30	0.66 ± 0.014	4.2×10^3
3-oxo-C8-HSL	6.2 ± 1.7	5.3 ± 2.1	1.2×10^3	8.5 ± 2.4	6.8 ± 2.6	1.2×10^3
C12-HSL	1.2 ± 0.071	0.049 ± 0.0085	2.5×10^4	1.3 ± 0.17	0.095 ± 0.029	1.3×10^4

[a] ND, no detectable activity. [b] Saturation kinetics could not be attained.

Table 3: Relative Catalytic Efficiencies (k_{cat}/K_M) of Site-Specific MCP Mutants to N266Y

	C4-HSL	C8-HSL	3-oxo-C8-HSL	C12-HSL
N266Y	1	1	1	1
wild-type MCP	ND[a]	0.13	0.033	0.25
N266F	0.26	0.41	0.31	0.43
N266A	0.91	0.69	0.19	0.32
N266C	0.56	0.29	0.14	0.55
N266M	0.85	0.11	0.13	0.51
N266S	0.59	0.49	0.12	0.47
N266T	0.66	0.26	0.12	0.25
A265G	ND	0.021	0.025	0.18
A265C	0.3	0.1	0.058	0.25
A265H	ND	0.016	0.0043	0.032
A265Y	ND	0.088	0.036	0.25

k_{cat}/K_M for AhlA and PPH toward C4-HSL were 1.5×10^5 M^{-1} s^{-1} and 3.0×10^4 M^{-1} s^{-1}, respectively (*5*)), we sought to increase the substrate range of wild-type MCP by grafting the loops at the C-terminal ends of the seventh and eighth β-strands of AhlA and PPH on to the MCP scaffold. With the expectation that the binuclear metal centers of MCP, AhlA, PPH, and SsoPox are essentially identical, we identified the specificity loops at the C-terminal ends of the seventh and eighth β-strands (Figure 3A) from a sequence alignment based upon the available structure of SsoPox (*14*), an orthologous member of the PLL group; the sequences of these loops are highlighted by the blue box in Figure 1. We constructed the MCP-AhlA and MCP-PPH chimeras and determined their reactivities with the various AHL substrates; the kinetic parameters of these MCP loop chimeras are detailed in Table 4. Detailed sequences of the MCP loop chimeras are provided in the Supporting Information.

While AhlA exhibited a proficient reactivity toward C4-HSL, the grafting of either or both of the $\beta\alpha$ loops at the C-terminal ends of the seventh and eighth β-strands, respectively, from AhlA to MCP, did not result in a change in the substrate preference toward the short-chain C4-HSL (likewise for wild-type MCP, the MCP-AhlA loop chimeras had no detectable activity toward C4-HSL). Although it has been suggested that the substrate specificities of $(\beta/\alpha)_8$-barrel-containing enzymes in the

Table 4: Kinetic Parameters of MCP Loop Chimeras

	MCP-AhlA-β7			MCP-AhlA-β8		
substrate	k_{cat} (s^{-1})	K_M (mM)	k_{cat}/K_M ($M^{-1}s^{-1}$)	k_{cat} (s^{-1})	K_M (mM)	k_{cat}/K_M ($M^{-1}s^{-1}$)
C4-HSL	ND[a]	ND	ND	ND	ND	ND
C6-HSL	ND	ND	ND	0.46 ± 0.17	4.1 ± 2.6	110
3-oxo-C6-HSL	ND	ND	ND	0.13 ± 0.05	2.3 ± 1.7	57
C7-HSL	[b]	[b]	78	0.59 ± 0.25	0.88 ± 0.67	670
C8-HSL	0.63 ± 0.11	0.89 ± 0.34	710	1.3 ± 0.2	0.52 ± 0.19	2.5×10^3
3-oxo-C8-HSL	[b]	[b]	62	2.5 ± 0.5	3.9 ± 1.3	640
C10-HSL	0.44 ± 0.07	0.14 ± 0.05	3.1×10^3	0.8 ± 0.2	0.23 ± 0.14	3.5×10^3
C12-HSL	0.38 ± 0.04	0.09 ± 0.02	4.2×10^3	0.3 ± 0.05	0.08 ± 0.02	3.8×10^3

	MCP-AhlA-β7β8			MCP-PPH-β7		
substrate	k_{cat} (s^{-1})	K_M (mM)	k_{cat}/K_M ($M^{-1}s^{-1}$)	k_{cat} (s^{-1})	K_M (mM)	k_{cat}/K_M ($M^{-1}s^{-1}$)
C4-HSL	ND	ND	ND	ND	ND	ND
C6-HSL	[b]	[b]	4.8	[b]	[b]	25
3-oxo-C6-HSL	[b]	[b]	3.2	ND	ND	ND
C7-HSL	[b]	[b]	16	0.48 ± 0.07	3.4 ± 0.9	1.4×10^2
C8-HSL	0.11 ± 0.04	2.0 ± 1.2	55	0.79 ± 0.08	1.5 ± 0.3	5.3×10^2
3-oxo-C8-HSL	0.30 ± 0.14	5.8 ± 3.7	52	0.38 ± 0.03	2.0 ± 0.4	1.9×10^2
C10-HSL	[b]	[b]	120	[b]	[b]	1.4×10^3
C12-HSL	0.10 ± 0.04	0.20 ± 0.14	500	[b]	[b]	1.6×10^3

	MCP-PPH-β8			MCP-PPH-β7β8		
substrate	k_{cat} (s^{-1})	K_M (mM)	k_{cat}/K_M ($M^{-1}s^{-1}$)	k_{cat} (s^{-1})	K_M (mM)	k_{cat}/K_M ($M^{-1}s^{-1}$)
C4-HSL	[b]	[b]	17	[b]	[b]	33
C6-HSL	[b]	[b]	1.7×10^2	2.8 ± 0.7	2.6 ± 1.2	1.1×10^3
3-oxo-C6-HSL	[b]	[b]	29	[b]	[b]	66
C7-HSL	4.3 ± 1.1	2.7 ± 1.2	1.6×10^3	7.6 ± 1.4	2.5 ± 0.8	3.0×10^3
C8-HSL	7.5 ± 1.3	1.7 ± 0.5	4.4×10^3	5.0 ± 0.5	0.73 ± 0.19	6.8×10^3
3-oxo-C8-HSL	5.8 ± 1.9	4.2 ± 2.3	1.4×10^3	6.0 ± 0.7	2.3 ± 0.6	2.6×10^3
C10-HSL	[b]	[b]	6.3×10^3	[b]	[b]	8.0×10^3
C12-HSL	4.3 ± 0.7	0.7 ± 0.3	6.1×10^3	2.9 ± 1.4	0.28 ± 0.2	1.0×10^4

[a] ND, no detectable activity. [b] Saturation kinetics could not be attained.

amidohydrolase superfamily are inherently encoded within the $\beta\alpha$ loops at the C-terminal ends of the β-strands (*1*), we did not perform a grafting of all eight loops at the C-terminal ends of the β-strands because we were unsure of the additional complexities residing in the interfaces between the loops and central barrel and their effect on protein solubility and stability; in fact, we noticed that when both loops at the C-terminal ends of the seventh and eighth β-strands of AhlA were simultaneously grafted on to the MCP scaffold (MCP-AhlA-β7β8 chimera), the reactivities toward the various AHL substrates were reduced, relative to that of the wild-type enzyme. Thus, despite reports of successful loop swapping efforts that conferred new substrate specificities to old scaffolds, the effect of loop grafting is still both unpredictable and uncertain. A recent attempt by Raushel and co-workers to enhance phosphotriesterase activity in a nonquorum-quenching PLL from *Deinococcus radiodurans*, by grafting all eight $\beta\alpha$ loops at the C-terminal ends of the β-strands from PTE (from *Pseudomonas diminuta*), resulted in insoluble protein; after attempts to refold the insoluble protein, the resultant soluble chimera had no detectable phosphotriesterase activity (*16*).

We had modest success in our attempt to change the substrate specificity of MCP toward short-chain AHLs by grafting the $\beta\alpha$ loops at the C-terminal ends of the seventh and eighth β-strands from PPH to MCP; the values of k_{cat}/K_M for MCP-PPH-β8 and MCP-PPH-β7β8 toward C4-HSL were 17 and 33 M^{-1} s^{-1}, respectively. For ease of comparison, we have listed the fold-differences in catalytic efficiencies (k_{cat}/K_M) of the MCP loop chimeras relative to that of the N266Y mutant in Table 5. We observed that when both loops at the C-terminal ends of the seventh and eighth β-strands of PPH were simultaneously grafted on to the MCP scaffold (MCP-PPH-β7β8 chimera), there was a change in AHL substrate preference favoring the shorter chain quorum molecules; loop grafting also resulted in a 3-fold increase in k_{cat}/K_M toward C4-HSL, relative to that of the N266Y mutant.

We sought to understand the basis for this change in substrate specificity. An inspection of the MCP-PPH-β7β8 chimera sequence against the wild-type enzyme revealed that there were five amino acid substitutions in the $\beta\alpha$ loops at the C-terminal ends of the seventh and eighth β-strands (residues highlighted in brown and green, respectively, in Figure 1). We noticed that the N266C mutation was among the three substitutions that resided in the loop at the C-terminal end of the eighth β-strand (Figure 3B); we had previously characterized the N266C mutant and found this mutation (along with six other possible substitutions at the 266 position) resulted in an increase in activity toward C4-HSL, relative to that of the wild-type enzyme. To further appreciate the contributions of these three substitutions, in the loop at the C-terminal end of the eighth β-strand, to C4-HSL activity, we constructed the Q279X/V280X site-specific random MCP library and screened for C4-HSL lactonase activity above that exhibited

Table 5: Relative Catalytic Efficiencies (k_{cat}/K_M) of MCP Loop Chimeras to N266Y

	C4-HSL	C6-HSL	3-oxo-C6-HSL	C7-HSL	C8-HSL	3-oxo-C8-HSL	C10-HSL	C12-HSL
N266Y	1	1	1	1	1	1	1	1
wild-type MCP	ND[a]	0.032	ND	0.14	0.13	0.033	0.12	0.25
MCP-AhlA-β7	ND	ND	ND	0.026	0.044	0.0063	0.055	0.079
MCP-AhlA-β8	ND	0.15	0.52	0.22	0.16	0.065	0.063	0.072
MCP-AhlA-β7β8	ND	0.0066	0.029	0.0053	0.0034	0.0053	0.0021	0.0094
MCP-PPH-β7	ND	0.034	ND	0.047	0.033	0.019	0.025	0.030
MCP-PPH-β8	1.5	0.23	0.26	0.53	0.28	0.14	0.11	0.12
MCP-PPH-β7β8	3	1.5	0.6	1.0	0.43	0.26	0.14	0.19

[a] ND, no detectable activity.

by the wild-type enzyme. Unfortunately, we were unable to find any mutants that had increased C4-HSL lactonase activity. From the *in silico* representation (Figure 3B), we expected the residues Q279 and V280 to be located further away from the active site, relative to the N266 position, and thus, these residues may not have as much a significant role as N266 in determining productive substrate-binding geometries or substrate specificity. Taken together, these observations suggested that the increased AHL lactonase activity toward C4-HSL was predominantly due to a suitable substitution (such as any of the seven mutations described in this study) at the 266 codon position of MCP.

Conclusions. MCP, from the PLL group of enzymes within the amidohydrolase superfamily, is a quorum-quenching lactonase that hydrolyzes medium to long-chain AHL molecules. Two other orthologous PLLs (PPH and AhlA, with 92% and 59% sequence identity to MCP, respectively) have been previously reported to exhibit broad-range specificities toward AHLs. Grafting of loops at the ends of the seventh and eighth β-strands (from PPH and AhlA, respectively) did not result in MCP loop chimeras with significantly improved *N*-acylhomoserine lactonase activity, nor increased AHL substrate promiscuity. Our observations are consistent with those of other laboratories using loop grafting in enzyme engineering, in that the effect of loop grafting is still both unpredictable and uncertain (*16*, *23*) . The quorum-quenching lactonase activity of MCP can be significantly enhanced by a single point mutation, N266Y, on the loop at the C-terminal end of the eighth β-strand. The substrate specificity of MCP can also be directed toward short-chain AHLs by the same point mutation. Our studies, along with reports by others, suggest that enhancement of enzyme activity can be brought about by subtle, remote changes that can favor productive geometries during catalysis. The number and chemical complexity of quorum molecules in the environment are both large and unknown, and tailoring the specificities of known quorum-quenching lactonases to other quorum molecules involved in microbial virulence and pathogenesis may be a challenging task; however, given the relative ease of activity enhancement and broadening of substrate range (brought about by a single point mutation on a loop remote from the central catalytic barrel), our findings not only reinforce the evolutionary potential of the $(\beta/\alpha)_8$-barrel fold but also suggest that quorum-quenching lactonases in the amidohydrolase superfamily can be used in future efforts to engineer biomolecules of therapeutic use.

ACKNOWLEDGMENT

We thank Professor John Gerlt for insightful discussions and Professor Frank Raushel for helpful information regarding enzymes from the amidohydrolase superfamily.

SUPPORTING INFORMATION AVAILABLE

The sequences of primers used in this study, a matrix of pairwise sequence identities between MCP and selected members of the amidohydrolase superfamily, the chemical structures of substrates used in this study, a typical screen containing colonies of transformants, and detailed sequences of the MCP loop chimeras. This material is available free of charge via the Internet at http://pubs.acs.org.

REFERENCES

1. Seibert, C. M., and Raushel, F. M. (2005) Structural and catalytic diversity within the amidohydrolase superfamily. *Biochemistry 44*, 6383–6391.
2. Gerlt, J. A., and Raushel, F. M. (2003) Evolution of function in (beta/alpha)8-barrel enzymes. *Curr. Opin. Chem. Biol. 7*, 252–264.
3. Holm, L., and Sander, C. (1997) An evolutionary treasure: unification of a broad set of amidohydrolases related to urease. *Proteins 28*, 72–82.
4. Pegg, S. C., Brown, S. D., Ojha, S., Seffernick, J., Meng, E. C., Morris, J. H., Chang, P. J., Huang, C. C., Ferrin, T. E., and Babbitt, P. C. (2006) Leveraging enzyme structure-function relationships for functional inference and experimental design: the structure-function linkage database. *Biochemistry 45*, 2545–2555.
5. Afriat, L., Roodveldt, C., Manco, G., and Tawfik, D. S. (2006) The latent promiscuity of newly identified microbial lactonases is linked to a recently diverged phosphotriesterase. *Biochemistry 45*, 13677–13686.
6. Camilli, A., and Bassler, B. L. (2006) Bacterial small-molecule signaling pathways. *Science 311*, 1113–1116.
7. Waters, C. M., and Bassler, B. L. (2005) Quorum sensing: cell-to-cell communication in bacteria. *Annu. Rev. Cell Dev. Biol. 21*, 319–346.
8. Dong, Y. H., Wang, L. H., Xu, J. L., Zhang, H. B., Zhang, X. F., and Zhang, L. H. (2001) Quenching quorum-sensing-dependent bacterial infection by an *N*-acyl homoserine lactonase. *Nature (London) 411*, 813–817.
9. Yew, W. S., and Gerlt, J. A. (2002) Utilization of L-ascorbate by Escherichia coli K-12: assignments of functions to products of the yjf-sga and yia-sgb operons. *J. Bacteriol. 184*, 302–306.
10. Chapman, E., and Wong, C. H. (2002) A pH sensitive colorometric assay for the high-throughput screening of enzyme inhibitors and substrates: a case study using kinases. *Bioorg. Med. Chem. 10*, 551–555.
11. Aubert, S. D., Li, Y., and Raushel, F. M. (2004) Mechanism for the hydrolysis of organophosphates by the bacterial phosphotriesterase. *Biochemistry 43*, 5707–5715.
12. Lindsay, A., and Ahmer, B. M. (2005) Effect of sdiA on biosensors of *N*-acylhomoserine lactones. *J. Bacteriol. 187*, 5054–5058.
13. Vick, J. E., Schmidt, D. M., and Gerlt, J. A. (2005) Evolutionary potential of (beta/alpha)8-barrels: in vitro enhancement of a "new" reaction in the enolase superfamily. *Biochemistry 44*, 11722–11729.
14. Elias, M., Dupuy, J., Merone, L., Mandrich, L., Porzio, E., Moniot, S., Rochu, D., Lecomte, C., Rossi, M., Masson, P., Manco, G., and Chabriere, E. (2008) Structural basis for natural lactonase and promiscuous phosphotriesterase activities. *J. Mol. Biol. 379*, 1017–1028.
15. Omburo, G. A., Kuo, J. M., Mullins, L. S., and Raushel, F. M. (1992) Characterization of the zinc binding site of bacterial phosphotriesterase. *J. Biol. Chem. 267*, 13278–13283.
16. Xiang, D., Kolb, P., Fedorov, A., Meier, M., Federov, E., Nguyen, T., Sterner, R., Almo, S., Shoichet, B., and Raushel, F. (2009) Functional annotation and three-dimensional structure of Dr0930 from

Deinococcus radiodurans: A close relative of phosphotriesterase in the amidohydrolase superfamily. *Biochemistry 48*, 2237–2247.
17. Neuenschwander, M., Butz, M., Heintz, C., Kast, P., and Hilvert, D. (2007) A simple selection strategy for evolving highly efficient enzymes. *Nature Biotechnol. 25*, 1145–1147.
18. Schmidt, D. M., Mundorff, E. C., Dojka, M., Bermudez, E., Ness, J. E., Govindarajan, S., Babbitt, P. C., Minshull, J., and Gerlt, J. A. (2003) Evolutionary potential of (beta/alpha)8-barrels: functional promiscuity produced by single substitutions in the enolase superfamily. *Biochemistry 42*, 8387–8393.
19. Wise, E. L., Yew, W. S., Akana, J., Gerlt, J. A., and Rayment, I. (2005) Evolution of enzymatic activities in the orotidine 5′-monophosphate decarboxylase suprafamily: structural basis for catalytic promiscuity in wild-type and designed mutants of 3-keto-L-gulonate 6-phosphate decarboxylase. *Biochemistry 44*, 1816–1823.
20. Yew, W. S., Akana, J., Wise, E. L., Rayment, I., and Gerlt, J. A. (2005) Evolution of enzymatic activities in the orotidine 5′-monophosphate decarboxylase suprafamily: enhancing the promiscuous D-arabino-hex-3-ulose 6-phosphate synthase reaction catalyzed by 3-keto-L-gulonate 6-phosphate decarboxylase. *Biochemistry 44*, 1807–1815.
21. Gerlt, J. A., and Babbitt, P. C. ((2009)) Enzyme (re)design: lessons from natural evolution and computation, *Curr. Opin. Chem. Biol.*, doi:10.1016/j.cbpa.2009.01.014.
22. Tawfik, D. S. (2006) Biochemistry. Loop grafting and the origins of enzyme species. *Science 311*, 475–476.
23. Ochoa-Leyva, A., Soberon, X., Sanchez, F., Arguello, M., Montero-Moran, G., and Saab-Rincon, G. (2009) Protein Design through Systematic Catalytic Loop Exchange in the (beta/alpha)(8) Fold. *J. Mol. Biol. 387*, 949–964.
24. Pettersen, E. F., Goddard, T. D., Huang, C. C., Couch, G. S., Greenblatt, D. M., Meng, E. C., and Ferrin, T. E. (2004) UCSF Chimera: A visualization system for exploratory research and analysis. *J. Comput. Chem. 25*, 1605–1612.